Science and Technology Infusion Climate Bulletin
NOAA's National Weather Service
42nd NOAA Annual Climate Diagnostics and Prediction Workshop
Norman, OK, 23-26 October 2017

Diagnosing Extreme Drought Characteristics Across the Globe

Ehsan Najafi[1, 2, 3], Indrani Pal[1, 2, 3], and Reza M. Khanbilvardi[1, 2, 3]

[1]*Department of Civil Engineering, City University of New York (City College), New York*
[2]*Center for Water Resources and Environmental Research (City Water Center), City University of New York (City College), New York*
[3]*NOAA-Cooperative Remote Sensing Science and Technology Center (NOAA-CREST), City University of New York, New York*

1. Introduction

Droughts are one of the world's most widespread climatic disasters having significant adverse impacts on every water-dependent sector and the economy. There is now higher confidence that extreme drought risk has been changing across the globe and will increase in the future with climate change. However, global extreme drought characteristics and their connections to regional as well as large scale climate have not been fully explored. In this study, considering extreme drought magnitudes and timing in every land region of the globe over the past several decades, we try to address the following research questions: 1- How have the annual extreme drought magnitudes changed across the globe? 2- What is the spatial distribution of extreme droughts in each continent? 3- Are there any joint dependencies between extreme droughts across the globe? Our preliminary analyses suggest that many parts of the world have experienced similar patterns in terms of extreme droughts.

2. Methodology and data

We implemented Palmer Drought Severity Index (PDSI) dataset from 1950 to 2014, as a popular drought indicator to diagnose its extreme characteristics. This index not only integrates precipitation and temperature but is also highly correlated with soil moisture content (Dai *et al.* 2004). PDSI has been successfully applied to quantify the severity of droughts across different climates (Wells *et al.* 2004). It ranges from about -10 (dry) to +10 (wet) with values below -3 representing severe to extreme drought. Gridded monthly self-calibrated PDSI, at 2.5-degree resolution, provided by NOAA/OAR/ESRL Physical Sciences Division (PSD) (http://www.esrl.noaa.gov/psd/), Boulder, Colorado, is used here.

Extracting relevant information hidden in the complex spatial–temporal drought data set is complicated. To identify spatial patterns, most famous statistical methods are based on the concept of intra- and intercluster variances (like the k-means algorithm) (Bernard *et al.* 2013). In terms of drought, clustering of extreme drought has been lacking. In order to cluster the extreme drought, we used PAM Algorithm along with F-madogram (Bernard *et al.* 2013). F-madogram measures the pairwise dependence between variable time series and can be used as distance matrix in the PAM clustering algorithm. The approach we used here, combines the PAM algorithm with the F-madogram and creates a simple clustering algorithm for maxima. This method generates clusters around the representative grid cells (medoids). In order to use this approach, we consider the minimum annual PDSI of each grid cell.

3. Results

Figure 1 (a) shows the significant trend of monthly PDSI data from 1950 to 2014. The slopes were computed based on the seasonal Kendall Trend Test considering the Serial Dependence. Approximately, longitudinally and latitudinally, we see that grids with negative slope outnumber the positive ones, which means in general, drought has become more severe during the last several decades. The African continent, eastern China, eastern Australia, western Canada, parts of Russia and Brazil have experienced more severe droughts. The US, western part of Australia and west of China, got generally less severe. Dipole patterns in

Correspondence to: Ehsan Najafi, 160 Convent Avenue, Steinman Hall 190, New York 10031;
E-mail: enajafi@ccny.cuny.edu

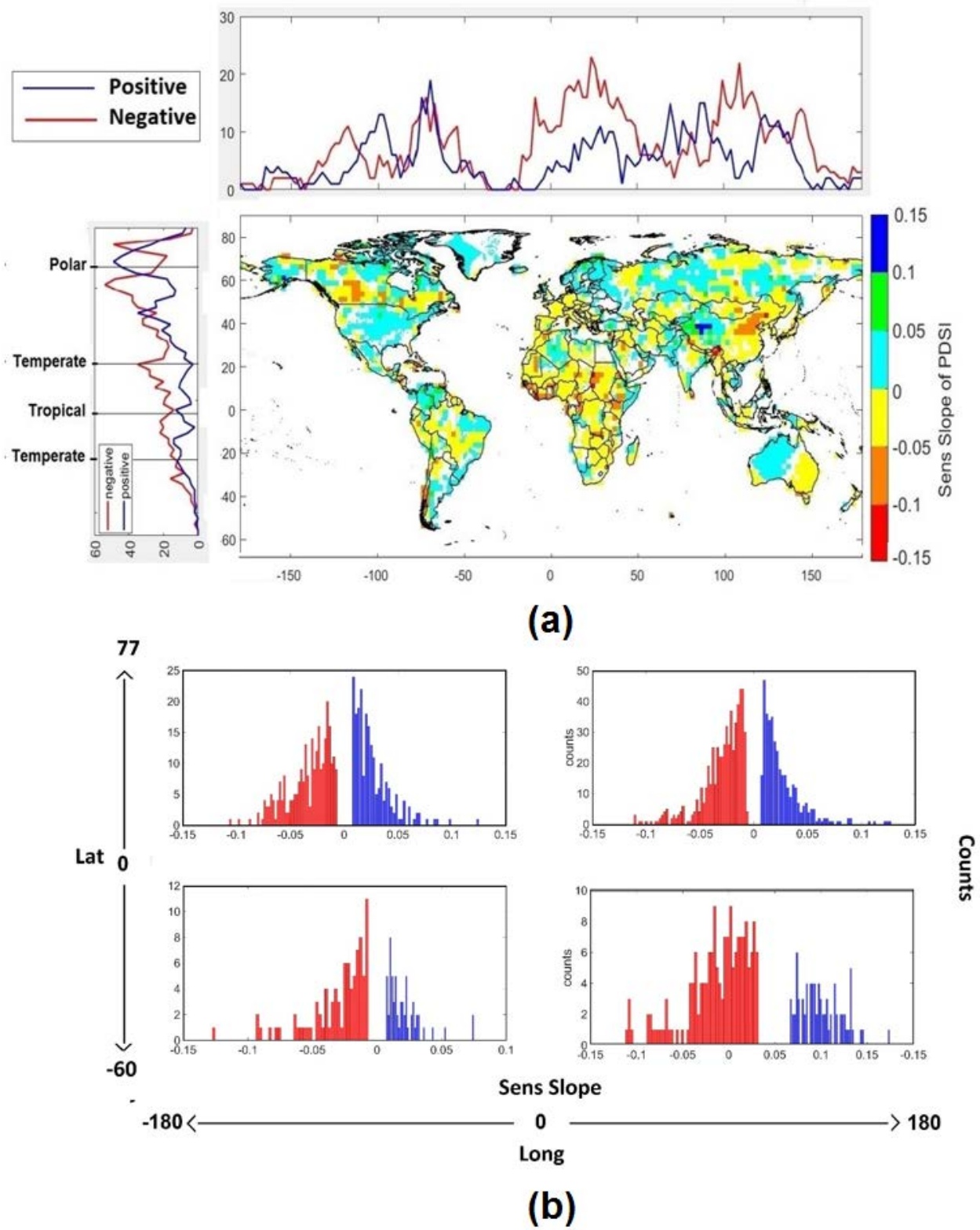

Fig. 1 (a) Trends (Sen's Slope) of Monthly PDSI from 1950 to 2014 (95% significance), and (b) slope distribution of monthly PDSI from 1950-2014 in four regions of the globe.

Australia and China are remarkable. One of the important features of this graph is that Africa has experienced more severe droughts through time during the last several decades. Using these maps, we will see that many of the continental clusters are categorized in the same location based on these trends. The slope distribution of

monthly and minimum annual PDSI in both latitude and longitude directions are shown in Figure 1 (b). It shows the slope distribution acquired from the previous step in 4 regions of the world. In general, the number of grids with negative slope outnumbers the positive ones.

Figure 2 represents the result of clustering for 6 continents. The number of clusters was defined based on the Silhouette Coefficient (SC) (Rousseeuw 1987). The medoids -that are the representative of each cluster- are shown by a pink diamond in each cluster and the PDSI trend of each cluster is shown under each continent's map. The trends of medoids are highlighted by a thick black color. In North America, the best number of clusters was found as 5. Clusters 2, 4 and 5 cover US and Mexico. Based on the trends of the medoids, it is clear that they are a good representative of each cluster. Interestingly South America is divided

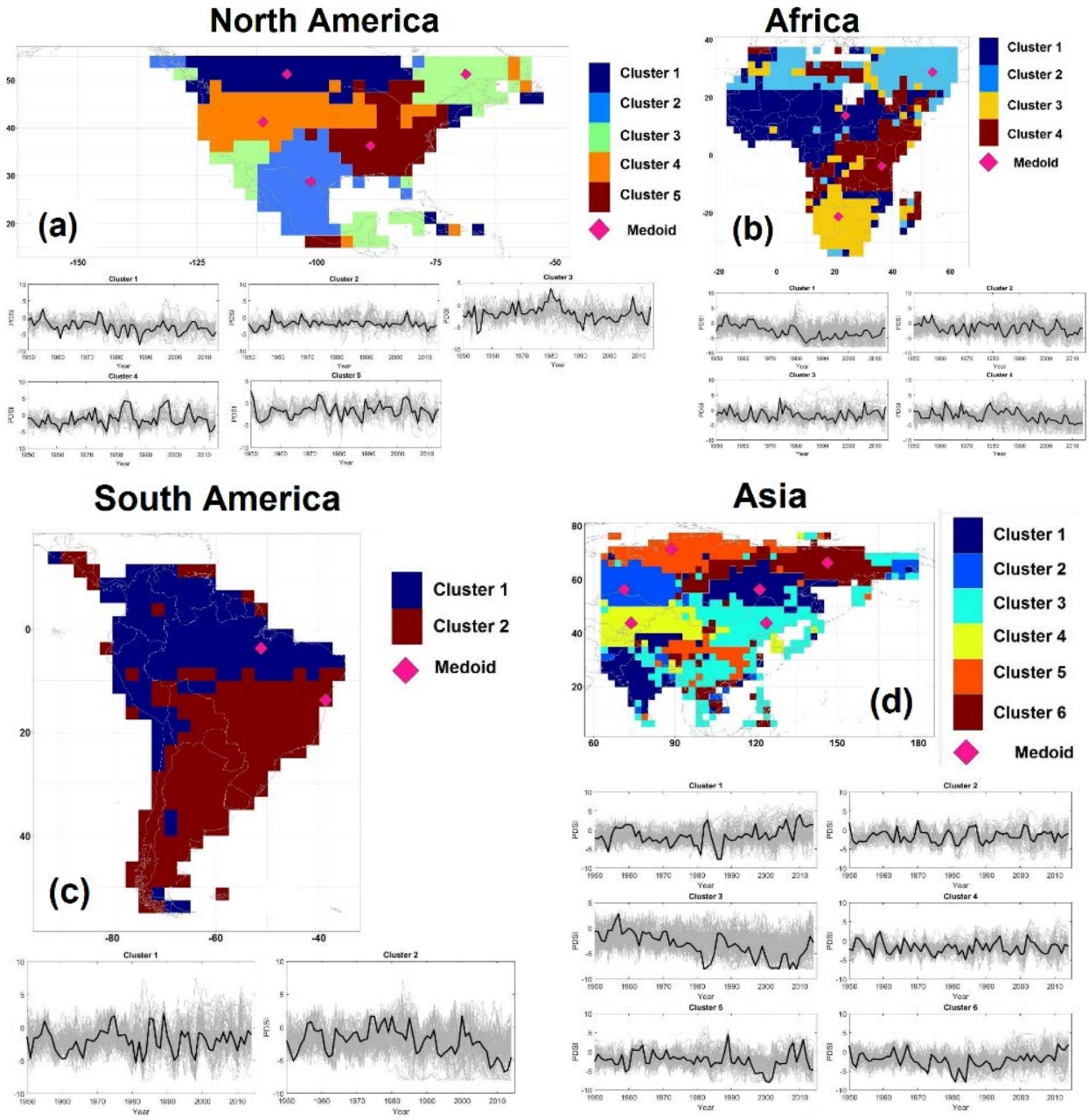

Fig. 2 The clusters of the annual extreme droughts over a) North America, b) Africa, c) South America, d) Asia, e) Oceania, and f) Europe from 1950 to 2014. In each map, medoids are shown by pink diamonds. The graphs depict the time series of PDSI for each cluster. The time series of the medoids are highlighted.

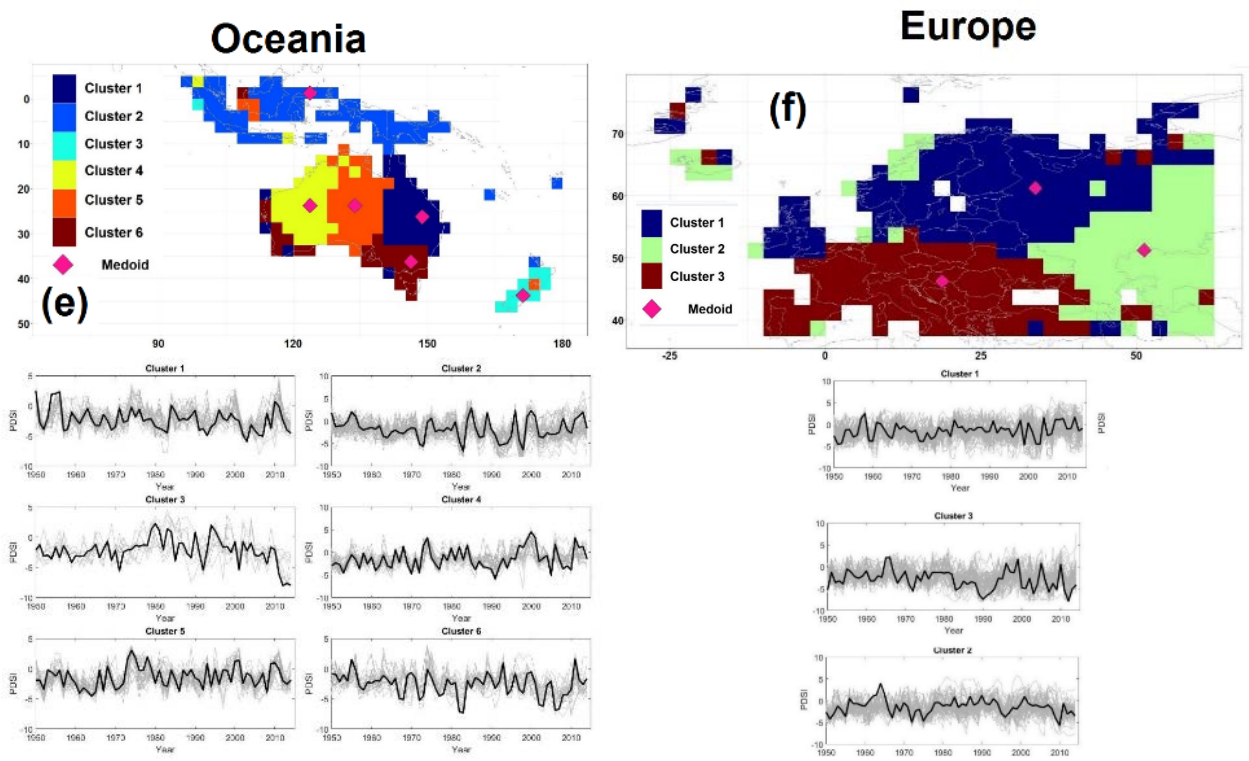

Fig. 2 (con't.)

into just two clusters in north and south and Europe and Africa are divided into 3 and 4 clusters respectively. In Asia, we found 6 clusters. Among all the continents, Asia contains the noisiest clusters, especially in the south (for example see the Cluster 3). This issue has been reflected in the time series of the medoids too. Based on Koppen climate classifications, there are many types of climatic regions in Asia and this might be one of the explanations of these noisy clusters. Unlike Asia, Oceania is very well classified. Australia is covered with 4 clusters; however, the cluster number 6 is a little noisy. New Zeeland and South Eastern Asian countries are all in one cluster.

Figure 3 presents the Spearman correlation between the medoids of all the clusters. The significant correlations are highlighted. The largest positive correlation belongs to cluster 3 of Asia and cluster 1 of Africa (0.58) and the largest negative correlation can be seen between cluster 3 of Oceania and cluster 6 of Asia (-0.5). In addition to these intercontinental correlations, there are significant correlations between clusters of each continent. For example, clusters 1 and 2 in Africa positively and clusters 1 and 3 in Europe negatively are correlated. The next step of this study will be examining the association between these clusters and climatic patterns such as sea surface temperature (SST). It should be noted that many problems are associated with some degrees of uncertainty, in these situations, the decision maker tries to find a solution that performs relatively well across uncertainties (Najafi *et al.* 2018; Afshar and Najafi 2014; Najafi and Afshar 2013; Armal *et al.* 2018). In the future, we will recognize and consider the uncertainties associated with the clustering as well as uncertainties between clusters and explanatory factors such as SST.

References

Afshar, A., and E. Najafi, 2014: Consequence management of chemical intrusion in water distribution networks under inexact scenarios. *J. Hydroinform.*, **16**, 178–188, DOI: 10.2166/hydro.2013.125

Armal, S., N. Devineni, and R. Khanbilvardi, 2018: Trends in extreme rainfall frequency in the contiguous United States: Attribution to climate change and climate variability modes. *J. Climate*, **31**, 369–385, https://doi.org/10.1175/JCLI-D-17-0106.1

Bernard, E., P. Naveau, M. Vrac, and O. Mestre, 2013: Clustering of maxima: Spatial dependencies among heavy rainfall in France. *J. Climate*, **26**, 7929–7937, https://doi.org/10.1175/JCLI-D-12-00836.1

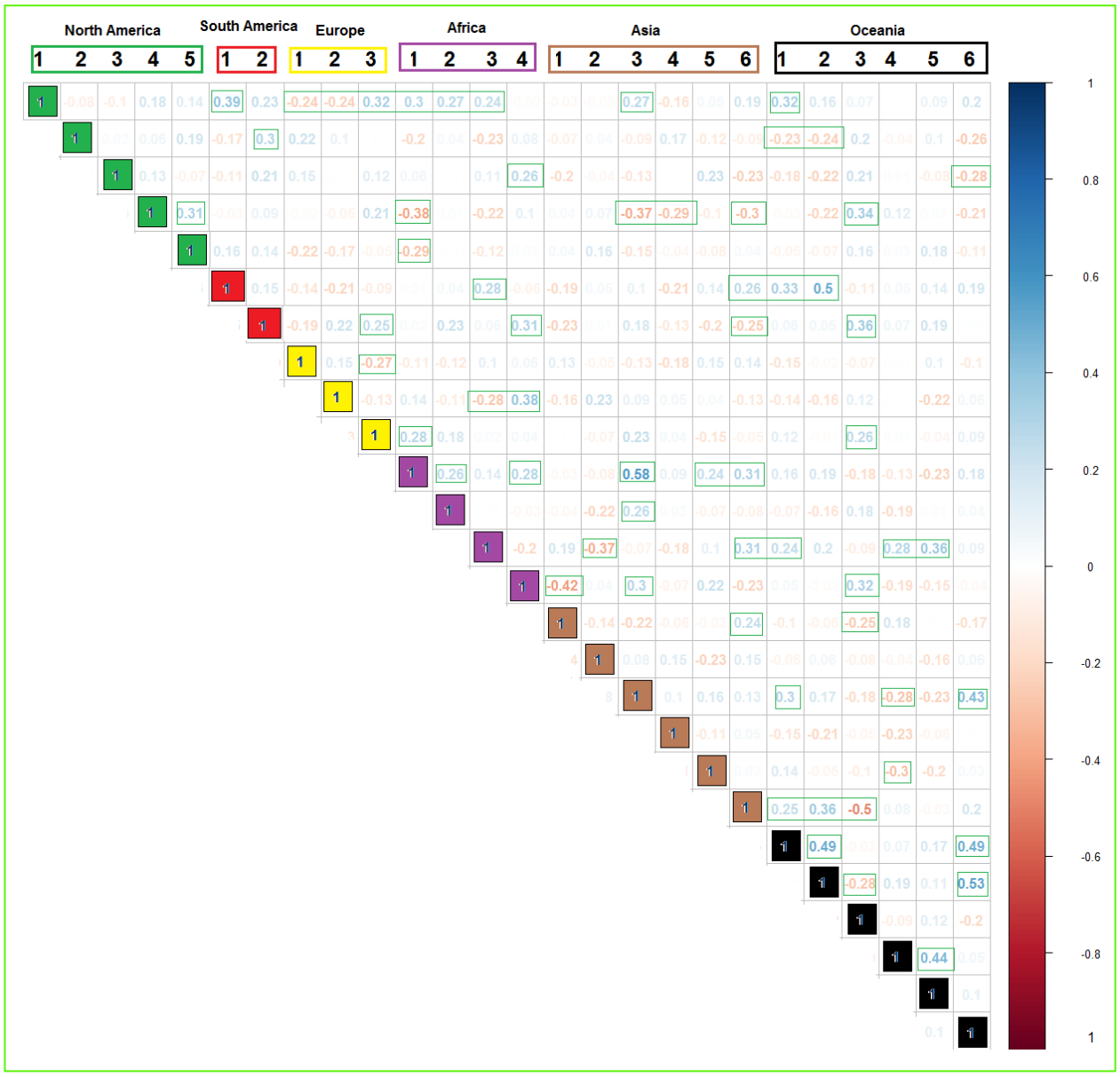

Fig. 3 The spearman correlation between medoids of all the clusters, the significant correlations are highlighted.

Dai, A., K. E. Trenberth, and T. Qian, 2004: A global dataset of palmer drought severity index for 1870–2002: Relationship with soil moisture and effects of surface warming, *J. Hydrometeorol.*, **5**, 1117–1130.

Najafi, E., and A. Afshar, 2013: Consequences management of chemical intrusions in urban water distribution networks using the ant colony optimization algorithm. *J. Water & Wastewater*, 82-94.

—, N. Devineni, R. M. Khanbilvardi, and F. Kogan, 2018: Understanding the changes in global crop yields through changes in climate and technology. *Earth's Future*, Accepted Author Manuscript. doi:10.1002/2017EF000690

Rousseeuw, P., 1987: Silhouettes: A graphical aid to the inter-pretation and validation of cluster analysis. *J. Comput. Appl. Math.*, **20**, 53–65.

Wells, N., S. Goddard, and M. J. Hayes, 2004: A self-calibrating palmer drought severity index. *J. Climate*, **17**, 2335–2351.